EUROPEAN ORGANIZATION FOR NUCLEAR RESEARCH

THE CROSS-SECTION FOR J/ψ PRODUCTION IN PROTON-PROTON COLLISIONS AT CENTRE-OF-MASS ENERGIES BETWEEN 23 AND 63 GeV

J.H. Cobb, S. Iwata*), R.B. Palmer, D.C. Rahm, I. Stumer
Brookhaven National Laboratory[1]),
Upton, New York, USA

C.W. Fabjan, I. Mannelli**), K. Nakamura***), A. Nappi**),
W. Struczinski†), W.J. Willis
CERN, Geneva, Switzerland

M. Goldberg, N. Horwitz, G.C. Moneti,
Syracuse University[2]),
Syracuse, New York, USA

C. Kourkoumelis, A.J. Lankford, P. Rehak††),
Yale University,
New Haven, Connecticut, USA

ABSTRACT

The cross-section for J/ψ production in proton-proton collisions has been measured as a function of centre-of-mass energy at the CERN Intersecting Storage Rings by observing its decay into electron-positron pairs. This cross-section is found to rise by a factor of about six over the full centre-of-mass energy range from $\sqrt{s}$ = 23 to $\sqrt{s}$ = 63 GeV. Electrons resulting from this decay were identified by the use of liquid argon calorimeters and lithium foil transition radiators. Measurements of the energies of the electrons were obtained from the liquid argon calorimeters.

Geneva - 28 January 1977

(Submitted to Physics Letters B)

---

*) Permanent address: Nagoya University, Nagoya, Japan.
**) On leave of absence from the University of Pisa and INFN Sezione di Pisa, Italy.
***) Permanent address: University of Tokyo, Tokyo, Japan.
†) Now at: Phys. Inst. T.H. Aachen, Aachen, Germany.
††) Now at: Brookhaven National Laboratory, Upton, NY, USA.
1) Research under the auspices of ERDA.
2) Work supported by the National Science Foundation.

We have measured the cross-section times branching ratio for the production of the J/ψ and its decay into electron-positron pairs over the full range of centre-of-mass energies available at the ISR and find that it rises by a factor of about six between $\sqrt{s}$ = 23 and $\sqrt{s}$ = 63 GeV.

The apparatus used is shown in Fig. 1. The J/ψ was observed by its decay into electron-positron pairs. The energies*) of the two electrons were measured in the segmented lead-liquid argon calorimeters [1] which also provided discrimination against hadron background. Additional electron-hadron discrimination was obtained by detecting, in xenon-filled proportional wire chambers [2], the transition radiation photons generated by the passage of the electrons through thin lithium foils. Cylindrical proportional wire chambers situated just outside the ISR vacuum chambers were used in order to reject electron pairs originating from photon conversions within the apparatus. Ionization-loss measurements made with two planes of scintillation counter hodoscopes allowed the elimination of Dalitz pairs, electron pairs originating from photon conversions in the vacuum chamber wall, and slow, heavily ionizing particles.

Two triggers were used concurrently to select events of interest. One, the "high-high" trigger, required that, in at least two of the four modules**) of the experiment, there appeared sufficiently energetic electromagnetic showers defined by simultaneous thresholds on the energy deposited in localized regions of the first 3.5 and the next 3 radiation lengths of the lead plate-liquid argon ion chamber. These thresholds were determined by the requirement that the trigger rate be acceptably low and, as a consequence, were such that the J/ψ was not recorded with full efficiency. The other trigger, "double-correlation", had considerably lower energy thresholds but required that a charged track was detected in the scintillation counter hodoscopes and second xenon chamber in spatial

---

*) The energy scale is calibrated such that the masses of the π^0, η, and J/ψ are consistent with their accepted values.

**) At times some modules were not active. Subsequent calculations of geometric efficiencies have taken this into account.

coincidence with the electromagnetic shower in the calorimeter. For the data reported herein these geometrical constraints were, however, such that again the J/ψ events were not recorded with maximum efficiency. The causes of the inefficiencies were quite different for the two triggers, but since the trigger conditions were recorded it was known for each event which trigger condition had been satisfied. Hence it was possible to use each trigger to determine the efficiency of the other. The combined trigger efficiency was about 50% at the J/ψ mass rising to 90% at high masses.

The segmentation of the liquid argon detectors into 20 mm wide strips running in three different directions allowed an unambiguous reconstruction of showers to be made. Four additional space points were measured for each charged track, two in the cylindrical proportional chambers and two in the xenon chambers. All of these used charge-division read-out to give the coordinate in the direction parallel to the beams.

Background to the true two-electron signal arises from hadrons interacting in the calorimeter, hadron tracks overlapping in the calorimeter with the electromagnetic showers of photons, and electrons originating from low-mass electron pairs. The trigger requirements and the calorimeter shower reconstruction procedure required that the longitudinal and radial distributions of deposited energy were characteristic of an electromagnetic shower and thus substantially reduced these backgrounds. In addition, the following requirements were imposed before a track was accepted as being an electron:

a) that the pulse height measured in the scintillator hodoscopes was less than 1.6 times that of a minimum ionizing particle;

b) that the transition radiation signal observed in the xenon chambers exceeded a threshold value (which was chosen such as to have an acceptance for electrons independent of their energy);

c) that, when associated with an electron candidate, no other shower gave an effective mass consistent with that of the π^0, and

d) that the electromagnetic shower lay in a certain, slightly restricted, fiducial volume of the calorimeter.

The selection of these requirements for background rejection was guided by exposures of a complete detector module to test beams of known particles, which also allowed the electron detection efficiency to be determined. It was subsequently found that when any one of the above requirements was released the J/ψ signal could still be observed and thereby it was possible to estimate the efficiency of each one using the actual data sample. The results of these two estimations were in satisfactory agreement. The greatest loss of real events was caused by the restriction on the scintillation counter pulse height but it was the most essential for eliminating background.

The efficiency of our reconstruction procedure was determined from a study of cosmic-ray muons and from inspection of event displays.

Figure 2a shows the distribution of the effective masses of pairs of electron candidates without the application of any of the above requirements (a, b, c, d). There is no sign of a J/ψ peak. Figures 2b to 2f show the mass distributions after these requirements have been made, for the total sample and for the samples at each centre-of-mass energy. There are clear J/ψ peaks with relatively little background. Two methods were employed to study the background. One method was based on the assumption that, with the above cuts, the single electron candidates were almost entirely composed of background (which we found to be true by comparison with the known single electron rates). Pairs of unrelated single electrons were combined to give a simulated electron pair mass spectrum. The other method was to use the shape of the distribution shown in Fig. 2a and to normalize it to the low mass region of the final mass spectrum shown in Fig. 2b. The results of these calculations agreed to within 20% implying that the background arises predominantly from uncorrelated pairs of misidentified particles. The second method was used for the background subtraction for the J/ψ cross-section.

The geometric and trigger acceptance of the apparatus for the J/ψ as a function of transverse momentum, p_T, and rapidity, y, was evaluated by means of a Monte Carlo program, assuming an isotropic decay. Comparing the distribution of observed events with the results of this calculation we find that the y-distribution is consistent with a constant value in the range $-0.65 \leq y \leq +0.65$. Then, assuming this distribution to be flat, the acceptance was integrated over y and used to correct the data as a function of p_T. It was found that $\langle p_T \rangle = 0.94 \pm 0.18$ GeV/c and that the data could be described by the form:

$$\frac{d\sigma}{dp_T^2} \propto e^{-bp_T} , \tag{1}$$

with $b = 2.1 \pm 0.4$.

The final acceptance calculation was performed using this distribution and the result is shown in Fig. 2g as a function of electron pair effective mass. The numbers of events between 2.75 and 3.45 GeV/c^2 were taken as the raw J/ψ signals and are given in Table 1, together with the integrated luminosities and cross-sections derived after background subtraction*). In addition to the statistical error, which is sufficient for comparing the cross-sections at the different centre-of-mass energies -- because the over-all efficiency should be substantially independent of $\sqrt{s}$ -- there is a scale error of a factor of about two which should be borne in mind when comparing these results with those of other experiments.

Figure 3 shows our results with the statistical errors only (the scale error being shown on the figure) together with a compilation of previous results [3]. The over-all agreement, in particular with the rather well determined values at Fermilab energies, is satisfactory. This newly demonstrated rise of the J/ψ production cross-section, which amounts to a factor of $5.41^{+5.0}_{-1.8}$ over the range of $\sqrt{s}$ covered by our experiment, agrees with the predictions of various theoretical models, in particular with that of the quark-antiquark fusion model of Donnachie and Landshoff [4], and in this framework provides a useful check of the quark distribution within the proton.

*) If a value of $b = 1.6$ is used for the P_T distribution assumed [Eq. (1)], then all cross-sections are increased by 12%.

REFERENCES

[1] W.J. Willis and V. Radeka, Nuclear Instrum. Methods 120 (1975) 221.

[2] J. Fisher et al., Nuclear Instrum. Methods 136 (1976) 19;

J.H. Cobb et al., Transition radiators for electron identification at the CERN ISR, to be published in Nuclear Instrum. Methods (1977).

[3] B.C. Brown et al., Study of J/ψ and ψ' production in proton-nucleus collisions with electron and muon pairs, FNAL preprint (1977).

See also:

J.J. Aubert et al., Phys. Rev. Letters 33 (1974) 1404.

Yu.M. Antipov et al., Phys. Letters 60B (1976) 309.

K.J. Anderson et al., Phys. Rev. Letters 36 (1976) 237.

H.D. Snyder et al., Phys. Rev. Letters 36 (1976) 1415.

F.W. Büsser et al., Phys. Letters 56B (1975) 482.

[4] A. Donnachie and P.V. Landshoff, Nuclear Phys. B112 (1976) 233.

Table 1

Numbers of events, integrated luminosities and J/ψ cross-section divided according to $\sqrt{s}$

$\sqrt{s}$ (GeV)	L (10^{36} cm^{-2})	Number of events	$B \times \left.\frac{d\sigma}{dy}\right\|_{y=0}$ (10^{-33} cm^2)	Statistical error (10^{-33} cm^2)	Absolute error (10^{-33} cm^2)
23	0.8	6	5.9	±2.4	±3.9
31	1.4	13	8.4	±2.3	±5.0
53	2.1	42	16.6	±2.6	±9.2
63	0.4	15	31.9	±8.2	±18.8

Figure captions

Fig. 1 : Vertical section of the apparatus transverse to the proton beams.

Fig. 2 : Distribution of effective masses of double electron candidates:

a) All.

b) After applying the requirements described in the text, then

c) to f) separated according to $\sqrt{s}$.

g) Relative efficiency of the apparatus as a function of m_{ee}.

Fig. 3 : $B(J/\psi \to e^+e^-) \times (d\sigma/dy|_{y=0})$ as a function of $\sqrt{s}$ compared with the results compiled in Ref. 3.

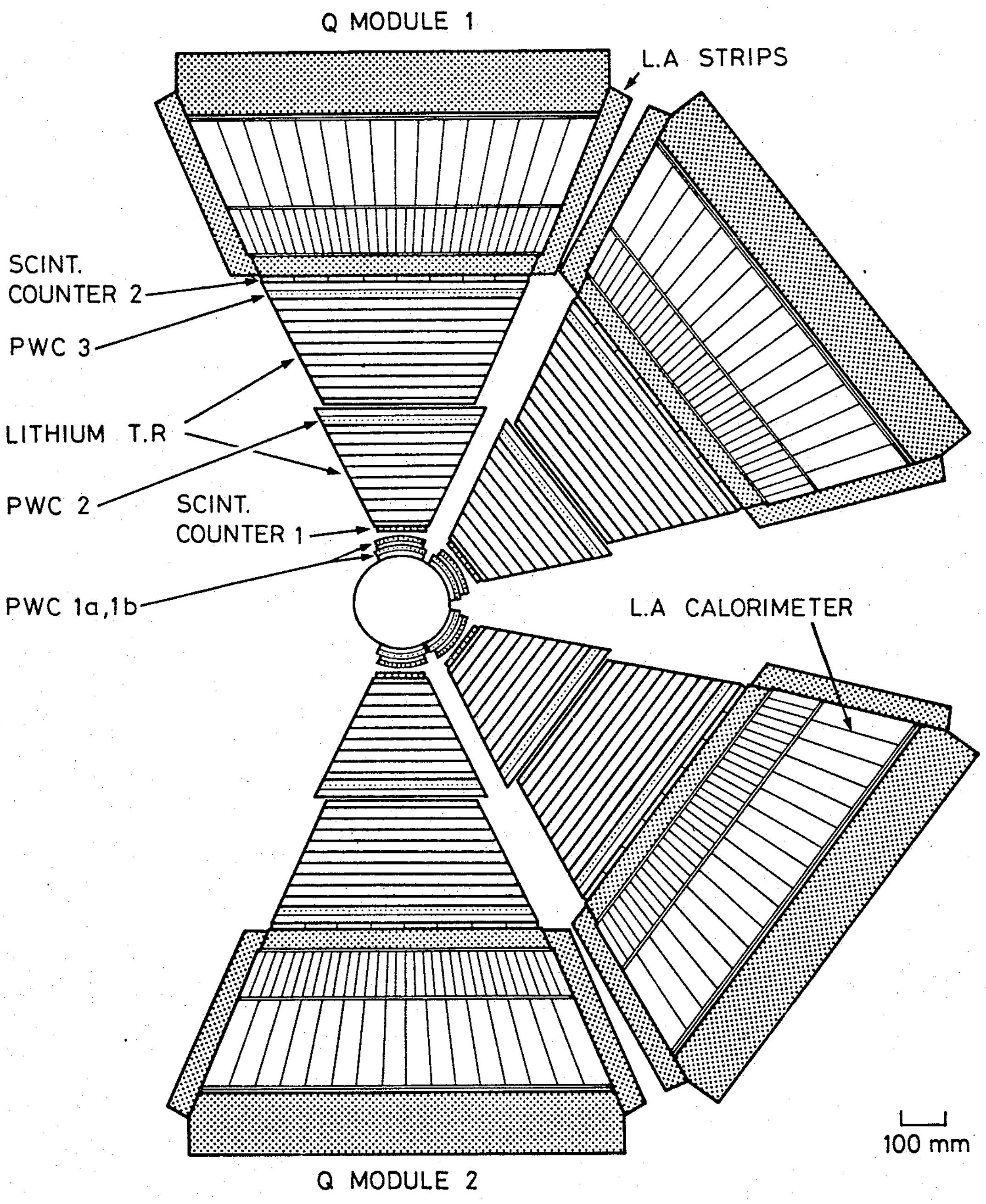
Q MODULE 1
L.A STRIPS
SCINT.
COUNTER 2
PWC 3
LITHIUM T.R
PWC 2
SCINT.
COUNTER 1
PWC 1a,1b
L.A CALORIMETER
100 mm
Q MODULE 2

Fig. 1

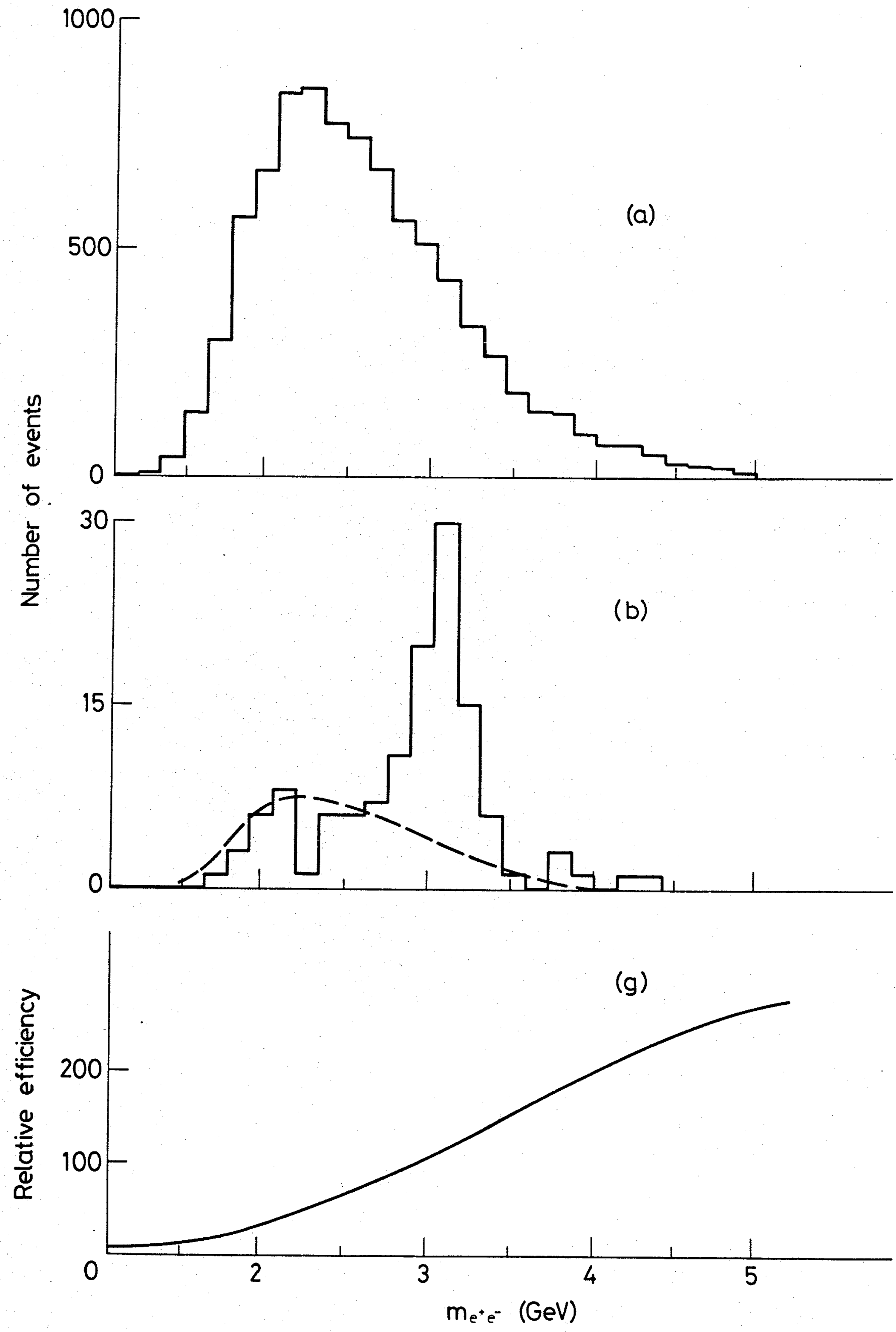
1000
500
0
(a)
Number of events
30
15
0
(b)
Relative efficiency
200
100
0
(g)
2
3
4
5
$m_{e^+e^-}$ (GeV)

Fig. 2

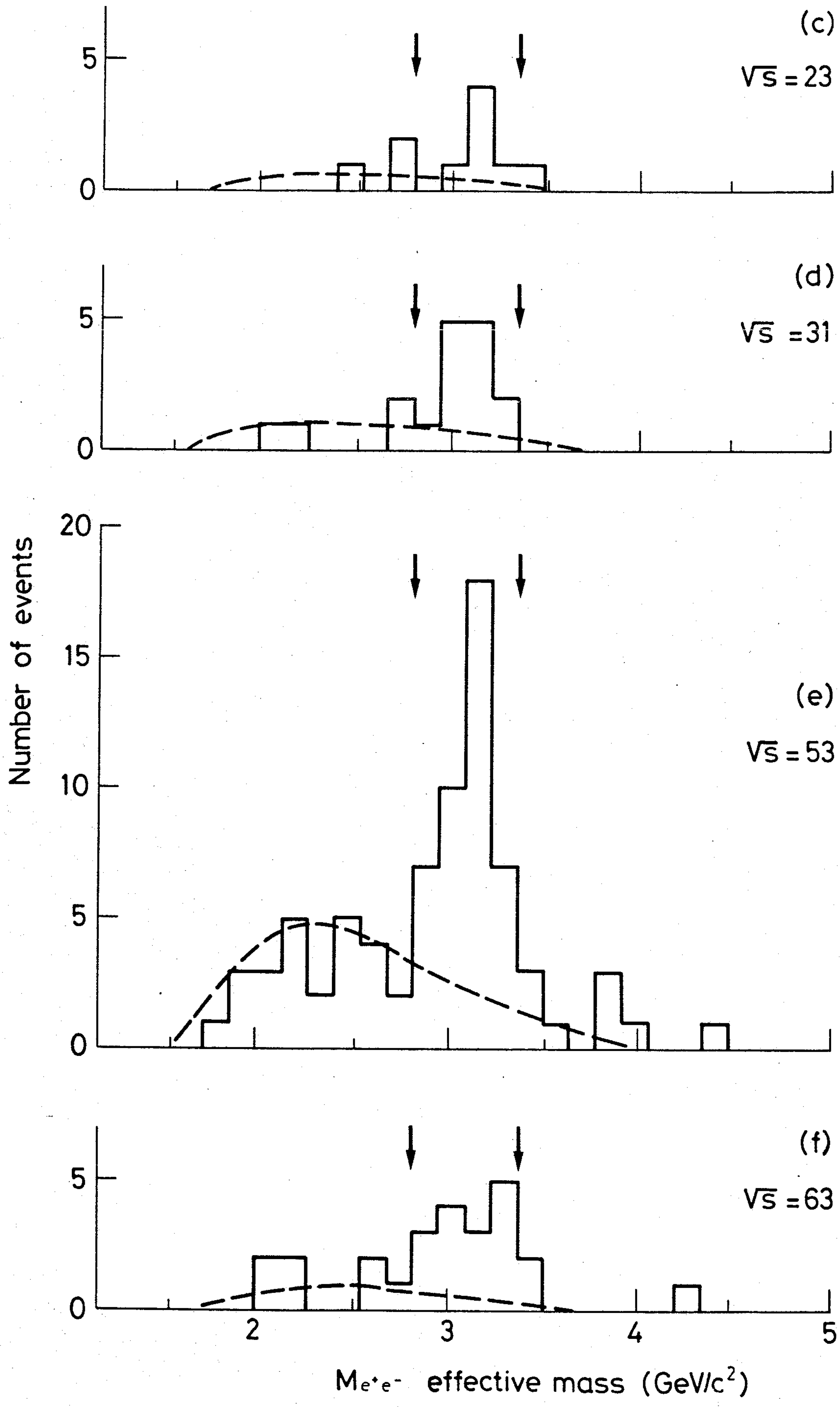

(c)
√s = 23
(d)
√s = 31
(e)
√s = 53
(f)
√s = 63
Number of events
0
5
10
15
20
2
3
4
5
Me+e- effective mass (GeV/c²)

Fig. 2

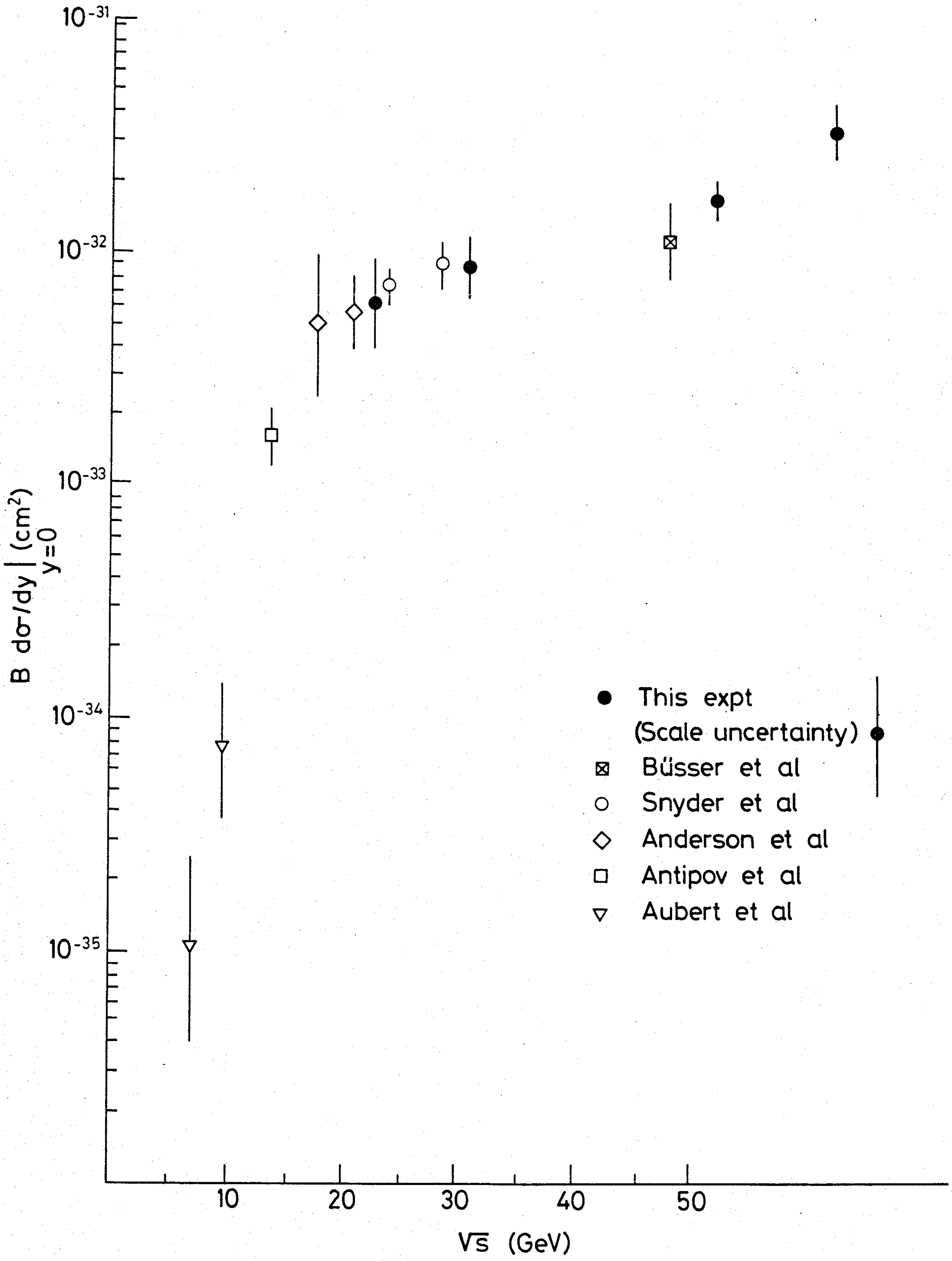

10^{-31}
10^{-32}
10^{-33}
10^{-34}
10^{-35}
B dσ/dy|$_{y=0}$ (cm^2)
This expt
(Scale uncertainty)
Büsser et al
Snyder et al
Anderson et al
Antipov et al
Aubert et al
10
20
30
40
50
√s (GeV)

Fig. 3